



Online and FREE access to plasma physics experiments

Pedro A. Mendes Rossa ,
Pavel Kurišćák ,
João N. Silva ,
José Veiga,
João P. S. Loureiro ,
João Oliveira ,
Daniel Hachmeister ,
Horácio Fernandes 

Abstract. Remote controlled laboratories had a great push during the COVID-19 pandemic. In fact, they were already out there but lacking in visibility. This external trigger pushed the academy to face a global challenge to start offering remote experiments more consistently and maturely. Instituto Superior Técnico (IST) has been offering several remote experiments since 2000 but with the need for an update due to technological aging. As such, the framework for remote experiments in education (FREE) was created based on new web technologies. In addition to the most diverse experiments that had already been developed, FREE includes two experiments that aimed at advanced-level physics students: the Langmuir probe and the electromagnetic (EM) cavity. Both allow users to configure the various parameters and to access the results in real time or check back later. All this access is done using a browser (on a PC or mobile phone) without the need to install additional software. The results of an experimental execution are stored in a database and are downloadable, allowing users to do various analyses and to determine the corresponding plasma density and temperature. In this paper, we will introduce how FREE was used in the implementation of both experiments and give an insight into their didactic approach, such as: (i) how to perform an experimental execution, (ii) the typical data set obtained with, and (iii) the corresponding analysis necessary for the user to retrieve information from it.

Keywords: Educational technology • E-lab • Electromagnetic cavity • Langmuir probe • Remote controlled experiments

P. A. Mendes Rossa , J. Veiga, J. P. S. Loureiro
Instituto Superior Técnico
Universidade de Lisboa, Portugal
E-mail: pedro.rossa@tecnico.ulisboa.pt

P. Kurišćák
Faculty of Nuclear Sciences and Physical Engineering
Czech Technical University in Prague, Czech Republic

J. N. Silva
Instituto Superior Técnico
Universidade de Lisboa, Portugal
and INESC-ID Instituto de Engenharia de Sistemas
e Computadores: Investigação e Desenvolvimento em
Lisboa, Portugal

J. Oliveira, D. Hachmeister, H. Fernandes
Instituto de Plasmas e Fusão Nuclear
Instituto Superior Técnico
Universidade de Lisboa, Portugal

Received: 31 August 2022

Accepted: 16 November 2022

0029-5922 © 2023 The Author(s). Published by the Institute of Nuclear Chemistry and Technology.
This is an open access article under the CC BY-NC-ND 4.0 licence (<http://creativecommons.org/licenses/by-nc-nd/4.0/>).

Introduction

Plasma is a difficult medium to handle and diagnose due to its very high natural temperature. Only refractory metals can be in direct contact with relatively cold plasmas allowing for direct readings of their properties. Conversely, most plasma diagnostics entail the only possibility of indirect measurements, either by emitted radiation or by the use of external sources. Based on this fact, e-lab presents two plasma experiments exemplifying this paradigm: (i) a Langmuir probe [1] where the voltage/current $I(V)$ characteristic is obtained with an immersive diagnostic and (ii) an electromagnetic (EM) cavity [2] that captures the EM properties of plasma in a non-invasive way.

Recently, e-lab [3] evolved to a web-based platform and these two experiments were the test beds within the advanced remote-controlled laboratory. This platform, the framework for remote experiments in education (FREE) [4], is being offered as open-source code and a plan is in place to migrate all e-lab laboratories to this new technology. Although a completely new underlying technology was used, the foundations and previous knowledge from the earlier e-lab developments were implemented following the same user approach.

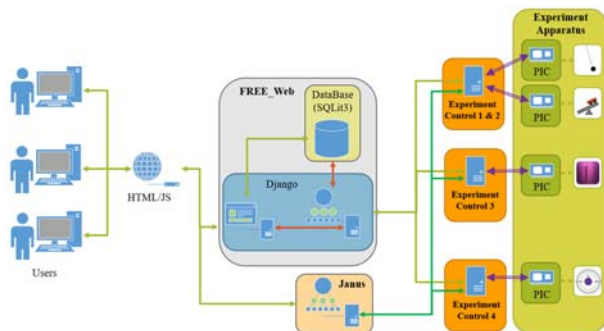


Fig. 1. Depicted FREE architecture where the central server acts as a broker between several users and the experiments with dedicated hardware, usually comprising a Linux proxy running in a Raspberry Pi and connected to the embedded system, custom made board with a PIC (peripheral interface controller), running a native C code.

This paper brings up an overview of the FREE framework and is followed by a description of how those two experiments were deployed in the e-lab advanced laboratory. We concluded with a brief report on the main results that can be obtained from these two experiments and how they compare between them.

FREE

The architecture of FREE is illustrated in Fig. 1, which is composed of a user interface (UI) that is presented as a webpage on a browser. The server implements a portal with a list of different experiments that the provider has and will provide access to them. The *Experiment control* is deployed on a computer close to the *Experiment apparatus*, like a simple Raspberry Pi.

After the decision to replace the remote experiment controller (ReC) platform and an evaluation of existing alternatives, a new remote laboratory supporting platform was designed and developed. All existing platforms [4] exhibit some limitations, which can be tackled and solved using modern and more suitable technologies and approaches. FREE

[4] was written in Python and Django and uses REST API [5] for all the communication between the UI (on a regular browser) and the physical experiment controller.

The project is developed and committed to a structured organization on GitHub, e-lab [6], where the code for the main server of FREE is published on the repository FREE_Web [7] and the *Experiment controller* is on the repository RPi_Proxy [8]. All code is open-source and, can be freely extended and integrated with existing experiments.

UI

When a user logs into e-lab [9], a list of all the experiments that are connected is presented, showing their corresponding status (offline or online), as shown in Fig. 2. If an apparatus can be used to do different experiments by selecting adequate experimental parameters, it is defined as a protocol. In this manner, the same apparatus can have different configurations and perform a variety of studies.

After choosing the desired *Apparatus type* and the *Protocol*, the FREE presents the user with a description of the *Apparatus type*, *Apparatus*, and *Protocol* containing the basic knowledge to understand the experiment (on the “Description” tab). Figure 3 presents an example of the page of the EM cavity.

On the “Configuration” tab, one can customize and save an execution by inputting the desired values into the box of the execution parameter (the box inside the blue square in Fig. 3a) and then pressing “Save”. By confirming the parameters, the execution can be inserted into a queue list of that *Apparatus* by pressing “Submit”.

Pressing the “Submit” button will move the webpage to the “Results” tab where, in real-time, the data collected from the experiment is displayed in a graph and on a table. It is also possible to observe the experiment in a window displaying a live video of the experiment (as shown in block of Fig. 3b).

List of Apparatuses

Apparatus type	Location	Scientific area	Lab type	Current status	Protocols
Pendulum	East Timor	Physics - Mechanics	Basic	● Online	Run Pendulum
Pendulum	Lisbon	Physics - Mechanics	Basic	● Offline	Run Pendulum
Langmuir	Lisbon	Plasma Physics	Advanced	● Online	Run Langmuir Elab
Cavity	Lisbon	Plasma Physics	Advanced	● Online	Run Cavity
Inclined Plane	Lisbon	Physics-Mechanics	Basic	● Offline	Run Inclined Plane Elab
Photovoltaic Panel	Lisbon	Energy	Basic	● Offline	Run Angle Sweeping Run Load Resistance
Pendulum	Oeiras	Physics - Mechanics	Basic	● Offline	Run Pendulum

Fig. 2. Screen capture from the main list of selected protocols, showing the available experimental protocols that can be executed in a particular apparatus.

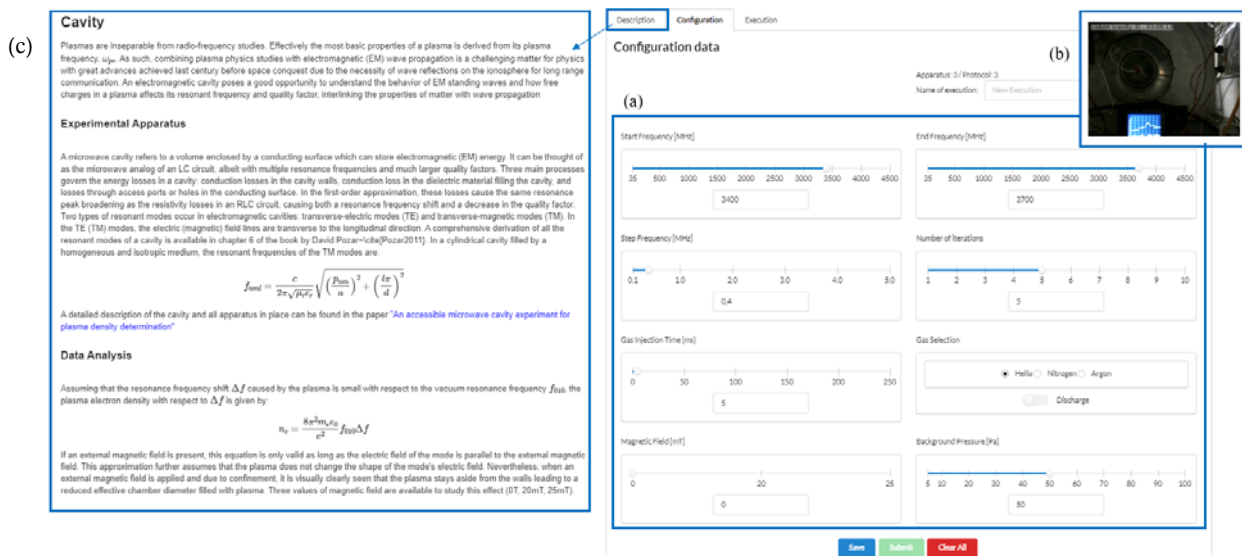


Fig. 3. The UI of the experiment EM cavity: (a) the configuration parameter to set your experiment, (b) the live stream of the experiment, and (c) framed by a brief description of the experiment.

Experiment control (RPI_Proxy)

The *Experiment control* is the piece of software in the FREE project that communicates with the FREE server and the experiment apparatus. To that end, it is actively seeking execution for the connected experimental apparatus from a user. This approach was chosen with security in mind for the FREE server, so it never initiates communication with *Experiment control*. Each time *Experiment control* requests a new execution, the FREE server checks its credentials against those registered in the database.

To make sure that the *Experiment control* is connected to the correct device the first thing it does is ask the FREE server to send it the necessary information to communicate with the experimental device and an identifier for it. Then, if everything is in order, the *Experiment control* is docked on the apparatus and begins the routine explained, as well as changing its status to online on the FREE UI.

Video stream

As was mentioned before, FREE supports the streaming of video from the apparatus to the user's browser. This is possible by having a camera facing the *Apparatus* and streaming the video via a streaming server (Janus [10] in the current version of FREE). When the user interacts with the webpage, it sends a request that is forwarded to the user's browser (using the Web Real-Time Communications (WebRTC) protocol [11]) starting the corresponding video stream.

Doing the streaming in this way relieves the user from the installation of video visualization software on their computer (as in the previous version of e-lab).

Presently, most videos are streamed using 640 × 480 resolution and 10 fps except in cases where a higher resolution or frame rate is specifically required given a particular image processing.

Experiments integration

The use of FREE and a supporting platform not only limits the types of interactions but also simplifies the development of the UI and communication between the physical device and the server. Furthermore, the genericity of FREE offered a set of features for free.

The only type of experimental interaction is as follows: (i) the user defined the parameters for the experiment execution and (ii) the experiment execution is set into a queue to be executed when the physical apparatus is available. At the moment the queue is a simple first-in-first-out without priorities and in the case of multiple concurrent users, there is a need to wait for each execution. This was a design decision when implementing FREE in contrast to the case where the user would reserve the physical apparatus for a certain amount of time to configure it and execute the experiments. Our solution seems to offer more fairness and simplifies the server's implementation. It also adds extra control over the number and frequency of experiments that a device can safely execute.

The development of the UI was also facilitated by the design of FREE. For each experiment, it was only necessary to use simple HTML (for the definition of the input fields and plot position) and a few JavaScript (JS) lines to update the plot. All other functionalities (such as argument verification and communication between browser and server is transparent to the programmer of these two experiments), so in total, the number of lines of code for the UI of these experiments is 154 HTML lines and 209 JS lines for the Langmuir probe and 152 lines of HTML and 118 lines of JS for the EM cavity.

The development of the communication between the experiment controller and the server is also simplified by the FREE architecture and design. All communications are initiated by the experiment controller acting as a pure client. When idle the experiment controller asks the server for the next experiment to

execute. During the experiments' execution, it is the controller that explicitly sends partial and final data to the server. Since this communication is performed using REST, with respect to network configuration, the controller only needs basic Internet access.

Langmuir probe

Plasma has a very high temperature (generally $>50\,000$ K), making it a difficult medium to accurately measure and characterize. Usually, this can be achieved by indirect measurements, based on its radiated light or its EM properties.

The Langmuir probe [12] is one of the few direct methods of plasma diagnostics and a simple one that allows for measuring some of these characteristics. The probe consists of a thin conductive wire immersed in the plasma. In a cold plasma, this perturbing object will collect mostly electrons, due to their higher mobility concerning ions, and become negatively charged, attaining a floating potential (V_f) if left floating. Usually, it will collect more electrons due to their mobility until it is sufficiently negatively biased for a null current flow due to electron repulsion.

If we bias the probe with a certain voltage (V_s), concerning the ground, we can either attract or repel the electrons in the plasma. By measuring the probe, I-V characteristic, that is, the relationship between the biasing voltage and the respective current going through the probe, one can extrapolate the electron temperature and density of the plasma.

If the biasing of the probe is negative enough, all the electrons will be repelled and the ion flux to the probe is almost independent of the applied potential. This is what we call the ion saturation current (i_{sat}^+) and it is described by Eq. (1) [being the current the total charge flow (j_{sat}^+) into the collection area of the probe (A_s)],

$$(1) \quad i_{\text{sat}}^+ = j_{\text{sat}}^+ A_s \approx \frac{1}{2} e n c_s A_s, \quad \text{with } c_s = \sqrt{\frac{kT_e}{M}}$$

where the flow of charge by the plasma density (n) times the plasma's speed of sound (c_s), being k the Boltzmann constant, T_e is the electron temperature and M is the ion mass.

There is a dependence between the collecting current and the biasing of the probe, as given by Eq. (2).

$$(2) \quad i^+ = i_{\text{sat}}^+ \left[1 - \alpha (V_s - V_f) \right]$$

This is due to an expansion of the sheath caused by increasing bias voltage. In such cases, the probe's electrical field is stronger and penetrates deeply into the plasma leading to an increased effective collection area. This dependence is almost linear and is taken into account by the α factor.

When decreasing the biasing voltage at some point, the electrons start reaching the probe (due to a reduction of sheath shielding), reducing the current. This singularity, where the characteristic detaches from the linear saturation current, gives the point where we observe an exponential behavior. The collected current is reduced by the emerging

electron current. This can happen even <0 V because of the electron's thermal energy.

Accounting for this balance we can retrieve the exponential behavior of the electrons due to their temperature, Eq. (3),

$$(3) \quad i = i_{\text{sat}}^+ \left(1 - e^{-\frac{e}{kT_e}(V_s - V_f)} \right)$$

this expression assumes that there is only one probe and that it is non-perturbative.

After a steep increase in the electron current, the plasma cannot continuously supply this avalanche of electrons. Then, we enter into the electron saturation current regime. This regime is not dictated by the electron temperature anymore, becoming almost linear, as in the ion case, but much steeper due to the electrons' mobility.

Experiment setup

The Langmuir probe used at the e-lab advanced laboratory is composed of the main chamber at the bottom of it. There is a modified ion gauge head from Edwards Vacuum that has two parallel plates, a thin tungsten filament, and a coil, as shown in Fig. 4.

The two parallel plates are connected to a high voltage (HV) radio frequency (RF) generator of approximately 50 kHz, which will generate the plasma. The thin tungsten filament is our Langmuir probe, which has 10 mm in length and a diameter of 0.2 mm, and the coil is used as a local ground.

To generate a vacuum there is a vacuum pump connected to the main chamber and to generate different types of plasma there are three cylinders (helium, argon, and xenon) connected to a gas injection system that is also connected to the main chamber. These two components are common to the EM cavity, as shown in Fig. 5. In particular, to reduce the flow of the gas valves a hollow needle was inserted into the valve connectors, as can be seen in Fig. 6. With this modification, we can have better control over the quantity of gas injected into the chambers of the experiments.

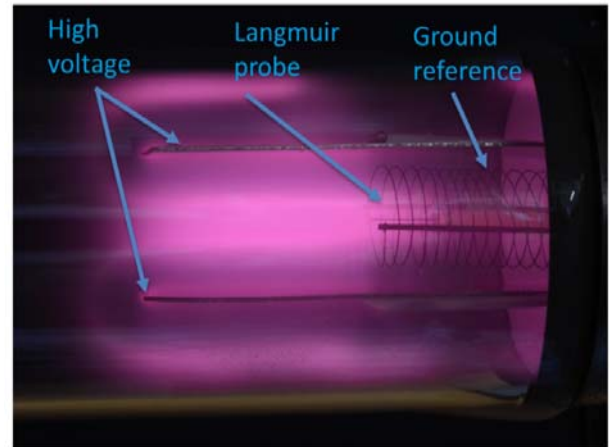


Fig. 4. Main components inside the chamber where the Langmuir probe is immersed and where the plasma is generated by a high AC voltage applied between the glow discharge molybdenum electrodes.



Fig. 5. Common rail vacuum system serves both experiments. On the left is the Langmuir probe and on the right is the EM cavity each with its own injection system but sharing the same gas rail. Only the EM cavity is equipped with magnetic field coils.



Fig. 6. The gas injection system was homemade with 200 μm clinical needles glued (epoxy) in the gas rail couplings.

The reading of the pressure inside the main chamber is done by a Pirani Gauge (PPT100) which is connected to a board that controls all experiments.

To function, the Langmuir probe needs a sweeping bias voltage. For this end, a message is sent with the frequency, peak-to-peak voltage (V_{pp}), and the type of wave (in this case a triangle wave), to the function generator (AD9850). In conjunction with an amplifier, driving an output transformer is to generate the bias voltage. To measure the probe characteristic, we use a PIC based custom-made board [1] with ADCs, and the corresponding electronics are used to provide offset adjustments and signal filtering.

Data collection and analysis

The data collected is grabbed in an elastic buffer. Initially, the sample rate is 1 sample/s and after reaching the preselected pressure, it is changed up to 1 k sample/s during the experiment.

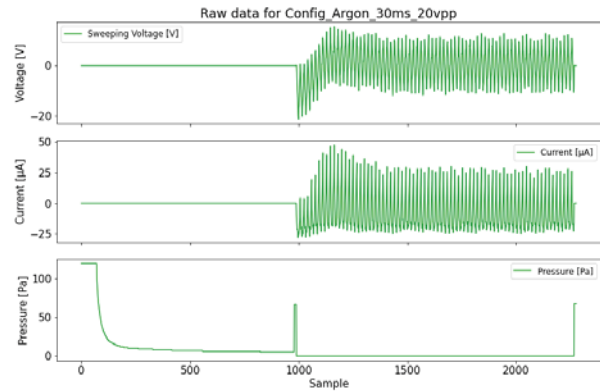


Fig. 7. Raw data from Langmuir probe displaying the initial electrical transient of the plasma. During the time period of the experiment, the pressure reading shows zero to identify the acquisition window.

The data collected by the Langmuir probe can be cumbersome and noisy (Fig. 7) due to the initial transient. A visual inspection of the data must be done to determine the relevant time interval to analyze.

The points corresponding to each half-period are identified and separated based on the direction of the sweep to verify the symmetry and hysteresis of the plasma response.

Parameters setting

In this experiment, the user can change the following parameters: sweeping voltage, period of the sweeping signal, number of samples per period, number of periods, background pressure, gas type, and injection time.

To generate plasma, it is important to have a low amount of gas in the chamber to allow for the plasma's existence; it is recommended to set a background pressure of < 15 Pa and set the injection time to open the valve for 25 ms to inject a suitable amount of gas. The density of neutrals achieved is an important factor and must be balanced between the critical points where the RF discharge can be sustained and the desired plasma density achieved. In RF or magnetron discharges a relatively high pressure needs to exist to allow the coupling between the EM energy and the molecular collisions that will ignite the plasma. As such the injection time window must be precise according (i) to the desired final pressure at which the experiment is to be performed and (ii) the gas used.

The other parameters are more related to the probe itself and the desired characteristic which relates to the acquisition procedure. These parameters are intended to allow various waveform and data sampling strategies according to the envisaged data analysis studies. Typically, for a well-defined $I(V)$ curve, the highest value for the points per period and a low frequency for the sweep signal should be chosen.

Because of the nature of the exponential region, a single sweep will lack data points.

Data analysis

By reducing the time window and plotting the data, it exhibits a clear lack of symmetry. Following its na-

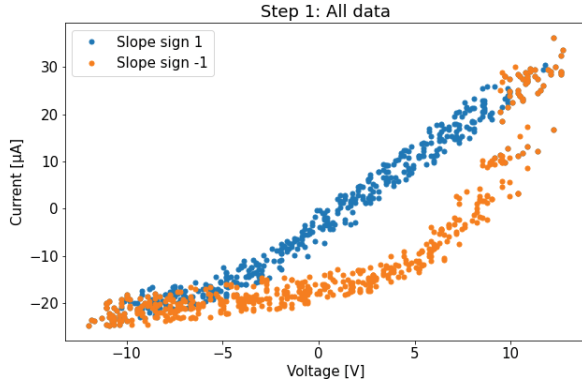


Fig. 8. Raw data from several sweeps displays a clear hysteresis when using a symmetrical triangular wave.

ture, the plasma will adapt to different spatial charges due to the probe potential, leading to an offset in the sensed potential. This result has a different characteristic according to the sweep direction, introducing a hysteresis effect which is clearly seen in Fig. 8.

We can also observe noise in the signal created by the intrinsic nature of the plasma RF generator. This induced noise can be mitigated by doing a proper average. Since we collected all the half-periods, we averaged the currents for a given voltage window.

As discussed earlier, we can identify the ion current region, fit it linearly and remove it from the data to simplify the characteristic, as shown in Fig. 9.

Nonetheless, the last points before the detachment correspond to the minimum sheath and are the ones that should be taken as the ion saturation current used to calculate the density, as displayed in Table 1.

Due to the exponential behavior that prompts us to perform a logarithmic scale transformation to identify the correct exponential window, as shown in Fig. 10.

On a logarithmic scale, we can see the detachment of the electron saturation current but be aware that log scales are very tricky to fool the eye and even more to the numerical fitting.

Table 1. Parameters obtained after the fitting shown in Fig. 9, the ion saturation current

Slope	$\alpha(1/V)$	V_f (V)	i_{sat}^+ (μA)
1	0.96	12.38	-17.2
-1	0.49	35.33	-17.6

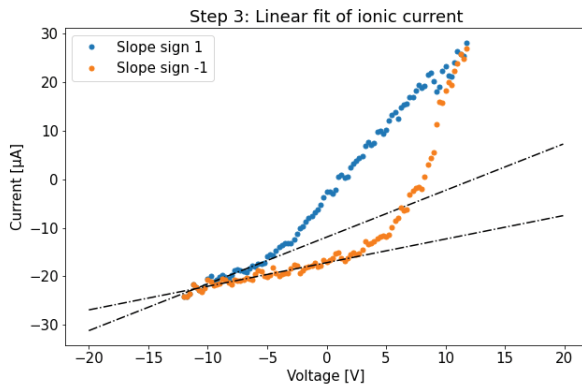


Fig. 9. Fitting of the ion saturation region, using Eq. (2), for correction of the data set.

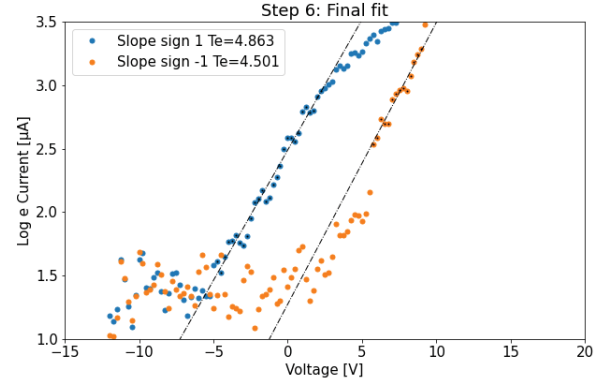


Fig. 10. By doing a semi-log graph, it is evident the exact location of the exponential part of the characteristic, and despite the lack of symmetry, the slopes are very similar in both situations.

Despite the existing hysteresis, the calculated temperatures retrieved from the data yield similar values as expected.

Taking the calculated electron temperatures, it is now possible to determine the sound speed, in which M is the mass of the ions, in this case, argon, so it gives us a sound speed of 3297 m/s allowing the determination of the density, using Eq. (1), which is about $n \approx 10.4 \times 10^{15} \text{ m}^{-3}$.

Results overview

It presented some results of execution done with the Langmuir probe, where the only parameter that was changed was the amount of neutral gas injected into the chamber, as shown in Table 2.

Evaluating the data, we can observe that in this region when we increase the pressure of neutral gas the density and the ion saturation current decrease and the electron temperature (and the speed of sound) stays approximately the same. With this, a conclusion can be made that the ion flux is reducing. This observation is expected and can be explained, and by increasing the pressure, we are reducing the mean free path of the particles, so a loss of energy due to the increase in the collision and consequent recombination of ion-electron pairs is expected.

EM cavity

An EM cavity can be seen as a portion of a waveguide and so the EM waveguide theory applies [13]. In a cylindrical cavity filled with a homogeneous and isotropic medium, the resonant frequencies of the transversal magnetic (TM) modes are given by Eq. (4).

Table 2. Results of multiple executions with different neutral gas pressure (Ar) and results for the ion saturation current, and the respective calculation of the speed of sound and the density

Pressure (Pa)	i_{sat}^+ (μgA)	T_e (eV)	c_s (m/s)	n ($\times 10^{15} \text{ m}^{-3}$)
64	-15.2	4.8	3405	8.9
100	-14.2	6.3	3901	7.2
150	-12.7	5.7	3711	6.8

$$(4) \quad f_{nml} = \frac{c}{2\pi\sqrt{\mu_r\epsilon_r}} \sqrt{\left(\frac{p_{nm}}{a}\right)^2 + \left(\frac{l\pi}{d}\right)^2}$$

The chosen mode to make this study was the TM_{010} due to no dependence on the z direction. Also, the electric field of this mode is parallel to the axial direction, while the magnetic field is parallel to the azimuthal direction, Fig. 11. Because of this, it is easily excitable by a loop antenna (magnetic antenna) with its axis in the azimuthal direction, instead of using a linear antenna that needs to be 1/4 of the wavelength and placed inside the plasma jeopardizing it. Note that the objective of this plasma diagnostic is to be a non-intrusive tool to measure the plasma parameter [14].

Since the EM cavity has a 32 mm radius the resonant frequency (f_{010}) is around 3586 MHz.

Plasma is an atmosphere of electrons and ions immersed in a neutral gas; therefore, it is an electrically conductive medium due to the presence of charged particles.

Since there are free charges, the propagation characteristics of the EM radiation change, and as such the solution of the wave equation yields the dispersion relation in the form of the Appleton–Hartree formula [15].

$$(5) \quad N^2 = 1 - \frac{2X(1-X)}{2(1-X) - Y^2 \sin^2 \theta \pm Z}$$

$$Z = \sqrt{Y^4 \sin^4 \theta + 4Y^2(1-X)^2 \cos^2 \theta}$$

Here, N represents the refraction index, and as a dependence on the plasma frequency ($X = (\omega_{pe}/\omega)^2$)

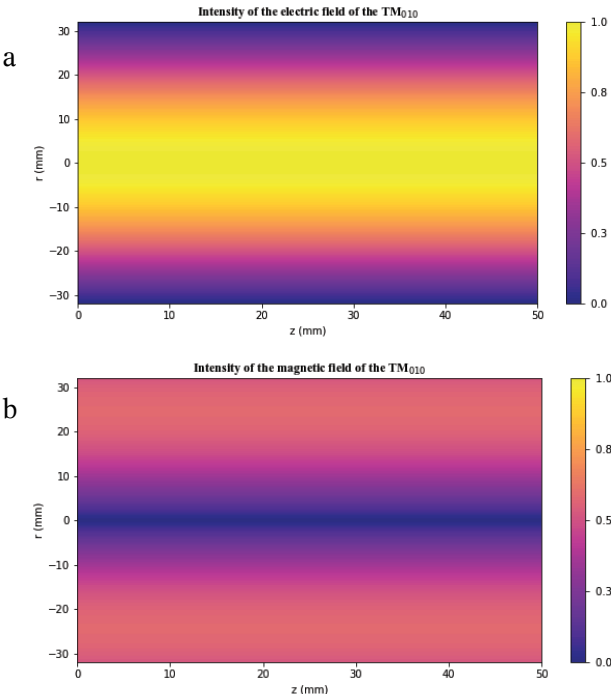


Fig. 11. Relative intensities of the electric field (a) and magnetic field (b) from an EM wave propagating in the TM_{010} mode. The electric field has a maximum in the middle of the cavity where the antenna must be inserted, jeopardizing the plasma. Conversely, in (b) the maximum is close to the walls where a magnetic antenna can be positioned to avoid disturbing the plasma and leading to the adopted solution.

and the cyclotronic frequency ($Y = \omega_c/\omega$ with $\omega_c = eB_0/m_e$) and θ is the angle between wave vector k and the external magnetic field B_0 . Moreover, the dielectric tensor can be simplified if the magnetic field is assumed to exist only in the ZZ axis, making the angle θ zero.

In the experimental setup, it is possible to change the plasma frequency and the cyclotronic frequency by changing the pressure and the intensity of the external field, respectively. There will always be a cross effect, as increasing the magnetic field alters the plasma density by capturing the electrons in the field lines, confining it, so a direct linear relationship cannot be expected.

A great simplification occurs if there is no external magnetic field, making the Appleton–Hartree to appear in the following form:

$$(6) \quad N^2 = 1 - \left(\frac{\omega_{pe}}{\omega}\right)^2$$

When the cavity is filled with a neutral gas, it has a resonant frequency of f_0 . This resonant frequency is shifted, from Δf to a new frequency f when the cavity is filled with a dielectric medium (plasma).

$$(7) \quad N^2 = \frac{f_0^2}{f^2} = \frac{\omega_0^2}{\omega^2}$$

By replacing this last result in Eq. (6),

$$n_e = \frac{\epsilon_0 m_e (\omega^2 - \omega_0^2)}{e^2} = \frac{4\pi^2 \epsilon_0 m_e}{e^2} (f^2 - f_0^2)$$

$$= \frac{4\pi^2 \epsilon_0 m_e}{e^2} ((f_0 + \Delta f)^2 - f_0^2)$$

we get the equation that relates the shift of the resonance frequency with the plasma density, Eq. (8)

$$(8) \quad n_e = \frac{8\pi^2 \epsilon_0 m_e}{e^2} f_0 \Delta f$$

Experimental setup

As mentioned before the vacuum system and the gas injection are shared with the Langmuir probe.

The main chamber is a cavity made from a nickel-plated copper body to protect it against corrosion, with a width of 64 mm in diameter and 50 mm in length, Fig. 12c. A cold cathode fluorescent light (CCFL) inverter serves as a current source to generate a Penning discharge inside the cavity. The HV inverter converts a ~ 12 V DC source to ~ 1 kV/50 kHz AC output which is applied between both electrodes inside the cavity.

These electrodes are copper-plated meshes, as shown in Fig. 12d, and are electrically insulated from the cylinder's lateral surface and close to the extremes of the cylinder seen in the figure. This configuration ensures that the discharge permeates the entire cavity uniformly.

The CCFL inverter managed to sustain discharges with working gas pressures between ~ 10 Pa and ~ 300 Pa. The whole cavity lies between two Helmholtz coils that generate a magnetic field of up to 25 mT, with a given ~ 1.4 mT/A on the coils.

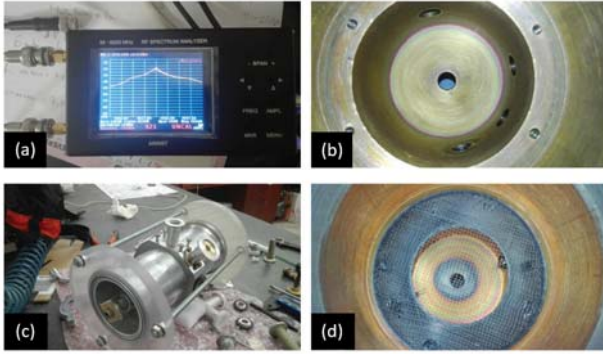


Fig. 12. Hardware parts from the EM cavity: (a) spectrum analyzer used, (b) the main cavity block, (c) assembly with the plexiglass windows on the top, and (d) ionizing HV electrode mesh with partial view of the loop antennas.

Two loop antennas lie in the middle of the cylinder wall opposing each other. The antennas have a ~ 4 mm radius with their axis coincident with the magnetic field line of highest intensity, the TM_{010} mode. One of the antennas injects the microwaves into the cavity, and the other antenna collects the propagated signal. An observed resonance is expected to be close to a frequency of 3560 MHz.

The main component of the diagnostic is shown in Fig. 12a, the spectrum analyzer (ARINST SSA-TG R2) allows scans in the range of 35–4500 MHz with a precision of 100 kHz.

Data collection and analysis

If we consider the spectrum analyzer that is being used, a broad-span scan done without plasma, Fig. 13, allows us to identify the main peak of the TM_{010} mode.

During the experiment we can see a slight pressure variation after the plasma ignition because some power is deposited on the neutral gas, leading to its heating and a corresponding neutral pressure increase.

By doing a broad span scan without plasma we can identify the main peak of the transverse magnetic mode 010.

Parameters setting

Users are allowed to configure the following parameters of the experiment: starting, ending, and step frequency of the acquisition of the spectrum; the number of spectrums to be collected; the background pressure; the injection time; and the type of gas that is injected; the intensity of the external magnetic field which activates the generation of the discharge (this allows the users to measure the resonant frequency of the cavity with no plasma).

It is important to (i) use enough large window of frequencies to observe the frequency shift and (ii) a sufficiently smaller frequency step to get more data points although this will reflect in a greater acquisition time.

To change the density of the plasma it is possible to increase/decrease the time that the gas injection valve is open (ranging between 0 ms and 250 ms). It is important to know that the injection time is not

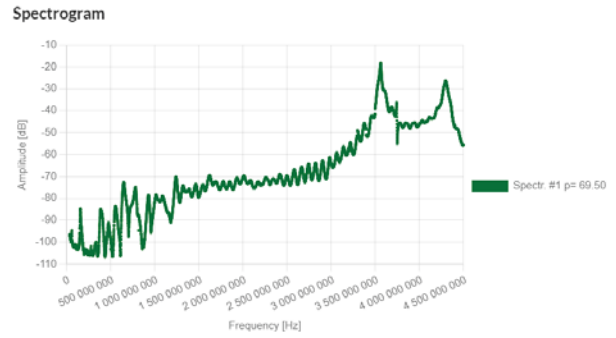


Fig. 13. Broad spectrum scan to identify the first resonant modes excited by the loop antenna.

linearly correlated to the pressure measured, so it is advisable to do a calibration set of experiments.

Data analysis

The simplest data analysis is to average the spectrums to mitigate the noise in the signal created by the RF generator.

With this initial data treatment, it is possible to accurately measure the peak frequency (f) and the width at -3 dB (δf) from where the quality factor is computed ($Q = f/\delta f$). It was chosen the reference at -3 dB from the peak's maximum value because the baseline noise level is never well-defined in RF measurements, and this is the main reason for considering the width at -3 dB instead of the width at half height.

In physics and engineering, the quality factor or Q factor is a dimensionless parameter that describes how underdamped an oscillator or resonator is. It is defined as the ratio between the initial energy stored in the resonator and the energy lost.

Figure 14 shows a proper fitting of the data. In this case, we analyze argon plasma, where we can detect the shift in frequency and the lowering in both the quality factor and the maximum intensity due to increased energy losses. These values can also be read by inspection of the figures. So, after analyzing the experimental data, we concluded that

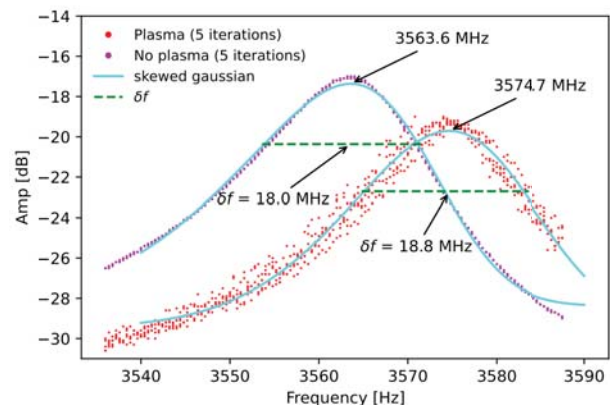


Fig. 14. The existence of plasma (Ar at 28 Pa) originates a drift on the resonant peak and a drop in the transmitted signal due to plasma losses and a consequent reduction in the quality factor.

the generated plasma had a density of $9.7 \times 10^{14} \text{ m}^{-3}$ ($\Delta f = 3574.5 - 3563.6 = 10.9 \text{ MHz}$) and a Q factor of about 198 and 190.1, respectively, resulting in a 4.0% reduction (Fig. 14).

Of course, a better estimation can be done mathematically by correlating the signals and extracting the frequency lag. Another reading from the correlation function is the similitude in the waveforms, allowing for accounting for the signal attenuation.

Results overview

It is presented with some results of execution done with the EM cavity, where the only parameter that was changed was the amount of neutral gas argon injected into the chamber, as shown in Table 3.

Looking at the data presented in Table 3 the first conclusion is that this experimental setup has a lower limit of 10 Pa for the neutral particles to be ionized corresponding to $\approx 0.7 \text{ mm}$ of mean free path (Fig. 15). Below that point, the CCFL cannot generate any plasma as it corresponds to the usual pressure limit of the Townsend discharge breakdown voltage where the avalanche process can no longer exist. From this point to the maximum plasma density achievable,

Table 3. Results of multiple executions with different neutral gas (Ar) pressures and the resultant frequency shift measured

Pressure injection (Pa)	f (MHz)	Δf (MHz)	n_e ($\times 10^{14} \text{ m}^{-3}$)
8	3563.6	–	–
10	3573.6	10.0	8.8
12	3580.8	17.2	15.2
13	3584.8	21.2	18.7
16	3586.4	22.8	20.2
18	3584.4	20.8	18.3
20	3582.5	18.9	16.7
21	3580.0	16.4	14.4
25	3578.4	14.8	13.1
28	3574.5	10.9	9.6
34	3572.8	9.2	8.1
44	3570.0	6.4	5.7
48	3568.8	5.2	4.6
60	3567.2	3.6	3.2
98	3566.8	3.2	2.8
120	3566.8	3.2	2.8

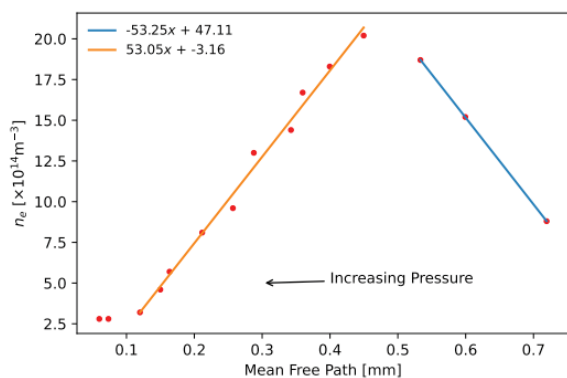


Fig. 15. Electron density in the function of the mean free path of the particles inside the chamber, as shown by data points in Table 3.

a constant raising of the electron density is visible, in a window of a few hundred microns, where the maximum relationship exists between the mean free path and the density. Here the density varies by one order of magnitude from the 0.1 mm reference. Then, due to the high pressure and the corresponding increase in the neutrals' density, the discharge's electron density is so low that the spectrometer cannot resolve the shift in frequency (0.1 MHz).

Conclusion

Both the Langmuir probe and the EM cavity are implementation paradigms of the open-source FREE. These experiments constitute the e-lab plasma advanced laboratory offered to the community by Instituto Superior Técnico (IST). The FREE infrastructure allows both real-time and offline data access to these experiments in a way that users can compare how invasive and non-invasive plasma experiments compare. Both experiments have been designed with a common rail gas injection and pumping system and both are equipped with the same ionizing source to make the experiments similar regarding the plasma source. It can be shown that the plasma density relates linearly with the mean free path between maximum density and the Townsend limits within the discharge existence.

To achieve very low pressures ($< 20 \text{ Pa}$) initially the vessel needs to be filled with a significant amount of the desired gas before the experiment. Then another execution is performed without gas injection and where the background pressure is used as a reference for the discharge.

Another important indication when doing a pressure sweeping is to do it from high pressures toward lower pressures to ensure less contamination from other gases used in previous experiments.

Overall, the plasma advanced laboratory requires a comprehensive knowledge of data analysis with different techniques and approaches that can be easily extended to other fields in physics.

Acknowledgments. This research has been supported by the Fusenet Association and co-funded by the Erasmus+ Programme of the European Union. It benefited from the IAEA support through a research agreement within the IAEA Research Contract No. 22750 on "Network of Small and Medium Size Magnetic Confinement Fusion Devices for Fusion Research". IPFN activities received financial support from "Fundação para a Ciência e Tecnologia" through projects UIDB/50010/2020 and UIDP/50010/2020.

ORCID

- H. Fernandes <http://orcid.org/0000-0001-6542-7767>
- D. Hachmeister <http://orcid.org/0000-0002-1420-4376>
- P. Kuriščák <http://orcid.org/0000-0002-2452-7187>
- J. P. S. Loureiro <http://orcid.org/0000-0002-7210-1025>
- P. A. Mendes Rossa <http://orcid.org/0000-0002-0139-1125>

J. Oliveira  <http://orcid.org/0000-0002-2784-214X>
 J. N. Silva  <http://orcid.org/0000-0002-7969-5487>

References

1. Loureiro, J. (2013). *Remote plasma experiments on e-lab*. Master dissertation, Instituto Superior Técnico, Universidade de Lisboa, Portugal, from <https://fenix.tecnico.ulisboa.pt/cursos/meft/dissertacao/2353642460043>.
2. Oliveira, J., Hachmeister, D., Lourenço, P. D., Bro-tankova, J., & Fernandes, H. (2021). An accessible microwave cavity experiment for plasma density determination. *Eur. J. Phys.*, *42*(3), 035203.
3. Instituto Superior Técnico. (2012). *E-lab. Remote laboratories*. Retrieved November 1, 2022, from <http://www.elab.ist.utl.pt>.
4. Kuriščák, P., Rossa, P., Fernandes, H., & Silva, J. N. (2022). Design and implementation of a framework for remote experiments in education. In 2022 VIII International Engineering, Science and Technology Conference, Panama, October 19–21, 2022, Panama City, Panama. DOI: 10.48550/arXiv.2211.01217.
5. Fielding, R. T. (2000). *REST: Architectural styles and the design of network-based software architectures*. Doctoral dissertation, University of California, from <https://www.ics.uci.edu/~fielding/pubs/dissertation/top.htm>.
6. Kuriščák, P., Rossa, P., & Silva, J. N. (2021). *FREE Project repository*. Retrieved November 1, 2022, from <https://github.com/e-lab-FREE>.
7. Kuriščák, P., Rossa, P., & Silva, J. N. (2021). *FREE main server repository*. Retrieved November 1, 2022, from https://github.com/e-lab-FREE/FREE_Web.
8. Kuriščák, P., Rossa, P., & Silva, J. N. (2021). *FREE experimental controller repository*. Retrieved November 1, 2022, from https://github.com/e-lab-FREE/RPi_Proxy.
9. Kuriščák, P., Rossa, P., Silva, J. N., Fernandes, H., & Veiga, J. (2022). *FREE e-lab*. Retrieved November 10, 2022, from <https://elab.vps.tecnico.ulisboa.pt:8000>.
10. Amirante, A., Castaldí, T., Miniero, L., & Romano, S. P. (2014, October). Janus: A general purpose WebRTC gateway. In Proceedings of the Conference on Principles, Systems and Applications of IP Telecommunications (pp. 1–8). USA: Association for Computing Machinery.
11. Sredojev, B., Samardzija, D., & Posarac, D. (2015, May). WebRTC technology overview and signaling solution design and implementation. In 38th International Convention on Information and Communication Technology, Electronics and Microelectronics (MIPRO) (pp. 1006–1009). USA: IEEE.
12. Hutchinson, I. H. (2002). Principles of plasma diagnostics. *Plasma Phys. Control. Fusion*, *44*(12), 2603.
13. Pozar, D. M. (2011). *Microwave engineering*. USA: John Wiley & Sons.
14. Luhmann, Jr. N. C., Bindslev, H., Park, H., Sanchez, J., Taylor, G., & Yu, C. X. (2008). Microwave diagnostics. *Fusion Sci. Technol.*, *53*(2), 335–396.
15. Bittencourt, J. A. (2004). *Fundamentals of plasma physics*. USA: Springer Science & Business Media.